Imprints on the CMB at low frequency & high resolution with the SKA

Carlo Burigana, INAF-IASF Bologna

First National Meeting on
Science and Technology with SKA
The Italian Pathway to SKA

Rome, 19-20 June 2012

Cosmic Microwave Background Radiation

Anisotropies

- $\frac{\Delta T}{T}(\hat{\mathbf{n}})$ → Angular power spectrum

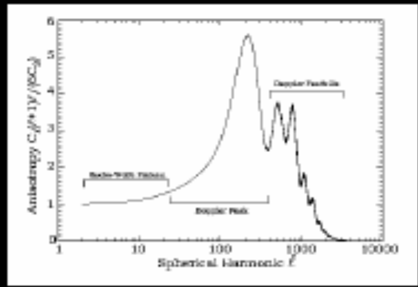

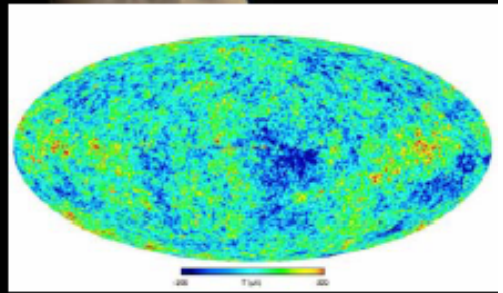

Polarization

- $\mathbf{P}^2 = \mathbf{Q}^2 + \mathbf{U}^2$ → Example:

  Scattering Thomson of radiation with quadrupole anisotropy generates linear polarization

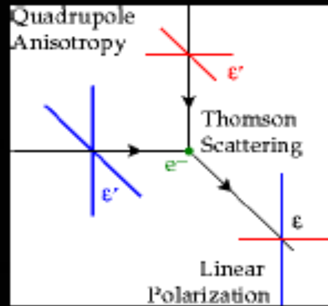

Spectrum

- Photon distribution function

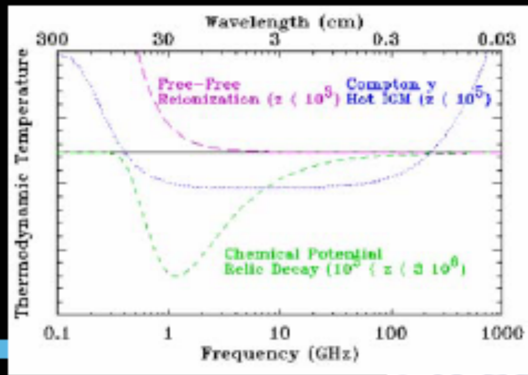

CMB after Planck satellite

- Polarization anisotropy
(ground & balloon, space missions, Moon-base):
  - E mode; TE mode: very accurate measures
  - B mode: detection? accurate measures?

- Spectral distortions
(ground & balloon, space missions, Moon-base):
  - Early & late processes: detection? measures?

- Very small scales (ground):
  - Secondary anisotropies / foregrounds
  - Statistical studies?
  - Detailed mapping

  → SKA will observe the very long wavelength tail of these CMB related themes

SKA ROLE to THE SUBJECT OF THIS PRESENTATION

CONTRIBUTIONS OF SKA ALONE?

Subrahmanyan R., Ekers R.D., 2002, in the XXVIIth General Assembly of the URSI, August 17-24, Maastricht, The Netherlands, astro-ph/0209569

CONTRIBUTIONS OF SKA ALONE VS. DEDICATED PROJECTS?

CMB experiments, Ryle Telescope (13m antennas, 15GHz), OVRO interferometer (10m antennas, 30GHz), BIMA array (6m antennas, 30GHz), AMI, SZA (antennas $\sim$ few $\times$ 100λ), ALMA ($\simeq$ PLANCK ν coverage, SKA resolution)

Jones M.E., 2003, in *The scientific promise of the Square Kilometer Array*, SKA Workshop, Oxford, 7 November 2002, eds. Kramer M., Rawlings S., pg. 47,

http://www.skatelescope.org/documents/

Workshop_Oxford2002.pdf

CONTRIBUTIONS OF SKA IN THE CONTEXT OF NEXT DECADE(S) PROJECTS?

This work

SKA contribution to CMB studies:

- Statistical analysis of Th. & Kin. SZ effect?
- SZ effect in AGN & protogalaxies (z up to ≈ 5)
- Free-Free emitters (z ≈ 10)
- Contribution to studies of CMB spectral distortions (z up to ≈ 10^7)
- Analysis of Galactic foregrounds

Thermal Sunyaev-Zeldovich effect

- Scattering of CMB photons with hot electrons
- Kompaneets equation formalisms but with

  $\int$ **c dt** → $\int$ **dl** → **L**

→ The effect is then proportional to the cluster (or hot gas halo) linear size

→The spectrum is exactly that of the Comptonization distortion (or small distortions in the case of warm gas) discussed above at least in the non relativistic limit

→Slightly different formalisms have been developed to deal with relativistic effects

N. of galaxy clusters: XMM ($\sim 10^3$), Planck ($\sim 10^4$), SDSS ($\sim 5\,10^5$)

Typical angular sizes of galaxy clusters: from $\sim$ arcmin to few tens of arcmin.

The SKA sensitivity and resolution mainly depends on the used array collecting area. Frequency band $\simeq 4$ GHz at 20 GHz.

Whole instrument collecting area (considering $\simeq 3000$ km maximum baseline) $\longrightarrow$ (rms) sensitivity of $\simeq 40$ nJy in one hour of integration with an angular resolution of $\simeq 1$ mas

50% of the collecting area within $\simeq 5$ km $\longrightarrow$ (rms) sensitivity in 1hour of integration is $\simeq 80$ nJy with a resolution of $\simeq 0.6''$.

With the 50% of the SKA collecting area it will be possible to accurately map the SZ effect of each considered cluster, particularly at moderately high redshifts, with an extremely precise subtraction of discrete radio sources.

Combination with X-ray images. Ex.:

Wide field imager (WFI) on board the X-ray Evolving Universe Spectroscopy (XEUS) satellite

(http://sci.esa.int/science-e/www/area/

index.cfm?fareaid=25)

by ESA: resolution of $0.25''$ on a FOV of $5' - 10'$.

Kinetic Sunyaev-Zeldovich effect

There is only one other mechanism leading to the "hole" in relic radiation. The receding of the cloud of electrons from the observer leads also to a decrease of relic radiation temperature in the direction of this cloud. The radiation temperature deficit is equal to

$$\frac{\Delta T_r}{T_r} \sim \tau_T \frac{v}{c} \cos\theta = \sigma_T N_e l \frac{v}{c} \cos\theta,$$

where v is the velocity of the cloud in the reference frame connected with relic radiation, θ is the angle between the velocity vector and the direction to the observer. The Doppler change of temperature does not depend on the frequency, contrary to the statement above (diffusion of the photons on the frequency axis due to scattering on hot electrons). Therefore it is possible to distinguish these effects observing the "hole" in the low-frequency, $h\nu < kT_r$, and high-frequency, $h\nu > kT_r$, parts of the spectrum.

Both effects are equal at

$$\frac{2kT_e}{m_e c^2} = \frac{v}{c}.$$

from Sunyaev-Zeldovich 1972

Let $I_0 = (2h_P/c^2)(k_B T_{CMB}/h)^3$; n_e=electron density; $x = h_P\nu/k_B T_{CMB}$=dimensionless photon frequency. Neglecting relativistic corrections (Zeldovich Ya.B., Sunyaev R.A., 1969, Ap. Space Sci., 4, 301):

$$\Delta I_{th} = I_0 y g(x) \quad (1)$$

$$\Delta I_k = -I_0 (V_r/c) \tau_e h(x)\,, \quad (2)$$

$$\tau_e = \int n_e \sigma_T dl \quad \text{Thomson optical depth} \quad (3)$$

$$y = \int (k_B T_e / m_e c^2) n_e \sigma_T dl \quad \text{Comptonization parameter} \quad (4)$$

$$h(x) = x^4 e^x / (e^x - 1)^2 \quad (5)$$

$$g(x) = h(x)[x(e^x + 1)/(e^x - 1) - 4]\,, \quad (6)$$

Different frequency dependence $\rightarrow$ separation through multi-frequency observations

SKA observations in the RJ regime (where $h(x) \sim g(x) \rightarrow x^2$) can be combined with mm observations ($g(x) \simeq 0$ and $h(x)$ is maximum at ~ 217 GHz)

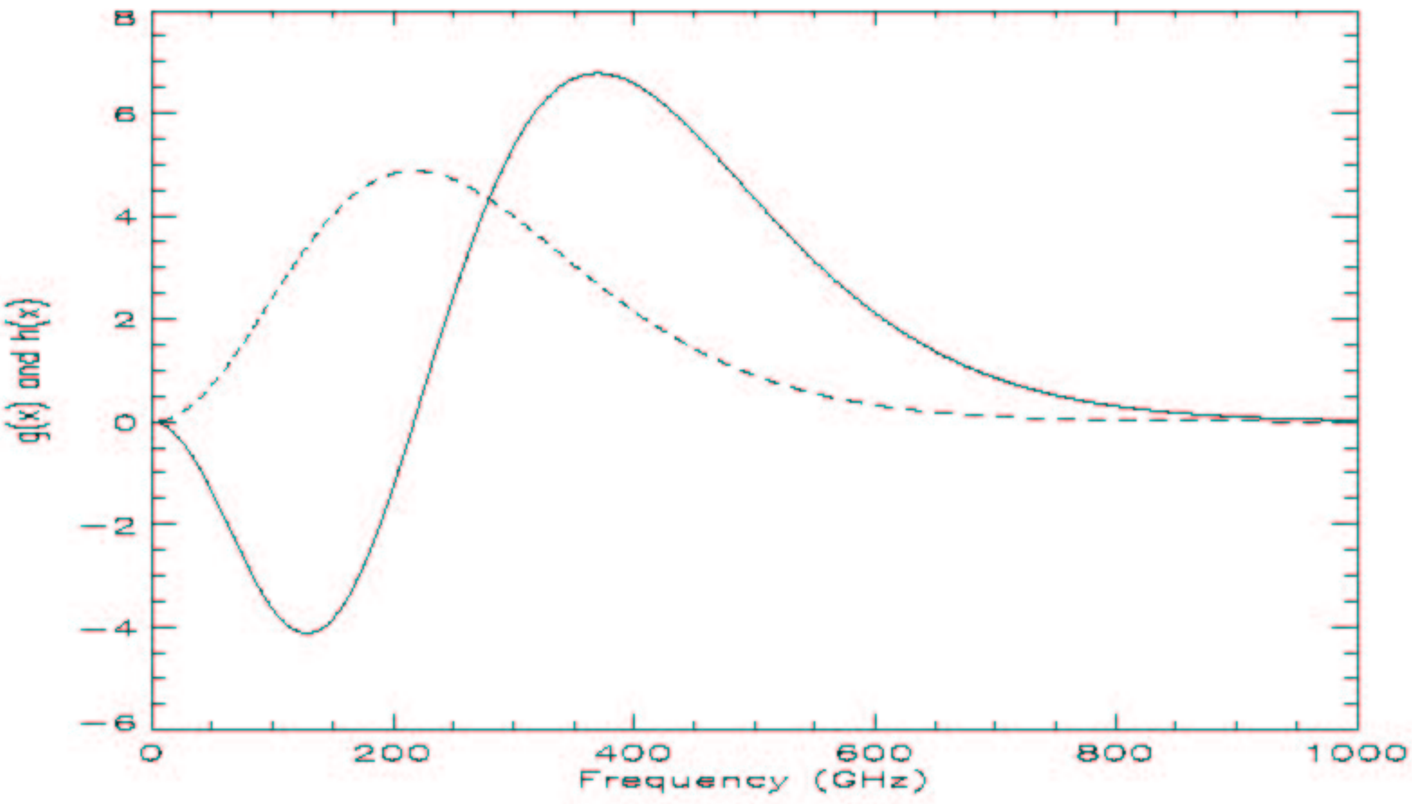

Functions g (solid line) and h (dashes) describing the frequency dependence of the thermal and kinetic SZ effect.

Radiosources in clusters - 1

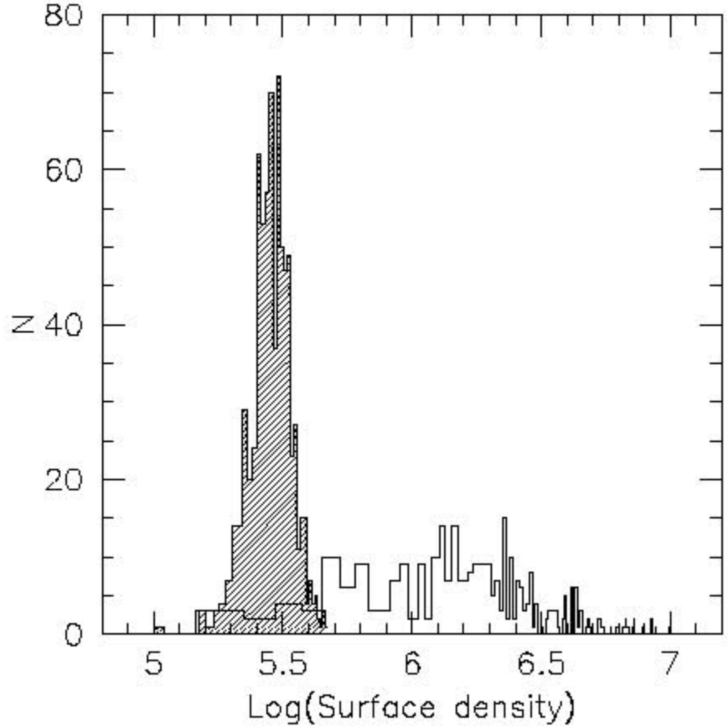

Fig. 1. Surface density (sr^{-1}) distribution of radio sources in the control fields (shaded area) and for clusters in the lowest redshift interval, within 0.25 Mpc from their centers.

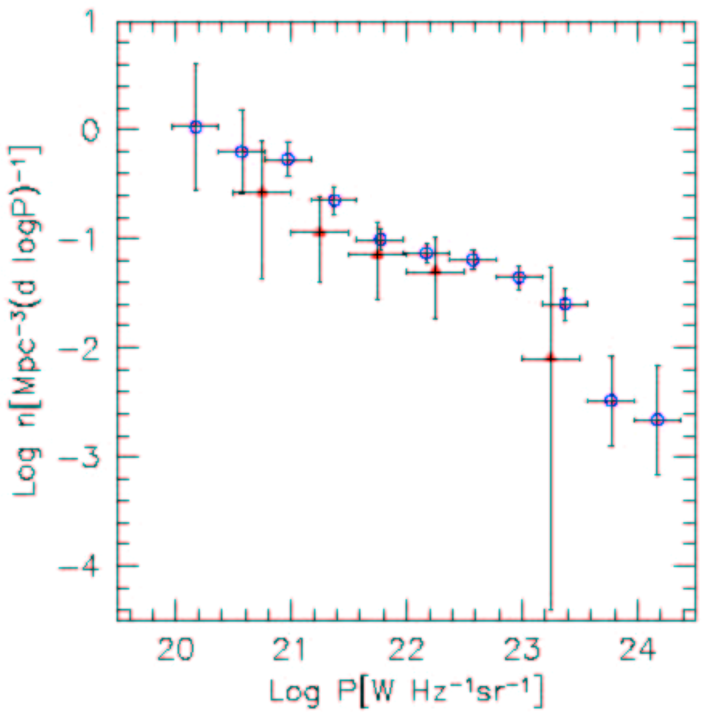

Fig. 5. Estimates of the luminosity function of cluster radio galaxies at 30 GHz. The open circles show the extrapolation to 30 GHz of the luminosity function in Fig. 4. The filled triangles represent our estimate based on the 30 GHz data by Cooray et al. (1998).

from Massardi & De Zotti 2004

Radiosources in clusters - 2

The contamination of the SZ effect by radio sources is more usefully expressed in terms of antenna temperature as:

$$\Delta T_A(\nu, z) = \frac{L_{\rm flat} + L_{\rm steep}}{2\pi k_b \lambda^2 r^2_{\rm cluster}(1+z)^3}, \qquad (3)$$

where $L_{\rm flat(steep)} = L_{\rm cluster, flat(steep), 1.4GHz}(\nu(1+z)/1.4{\rm GHz})^{-\bar{\alpha}_{\rm flat(steep)}}$, k_b is the Boltzmann constant and $r_{\rm cluster}$ is the physical radius of clusters, assumed here to be 1.73 Mpc.

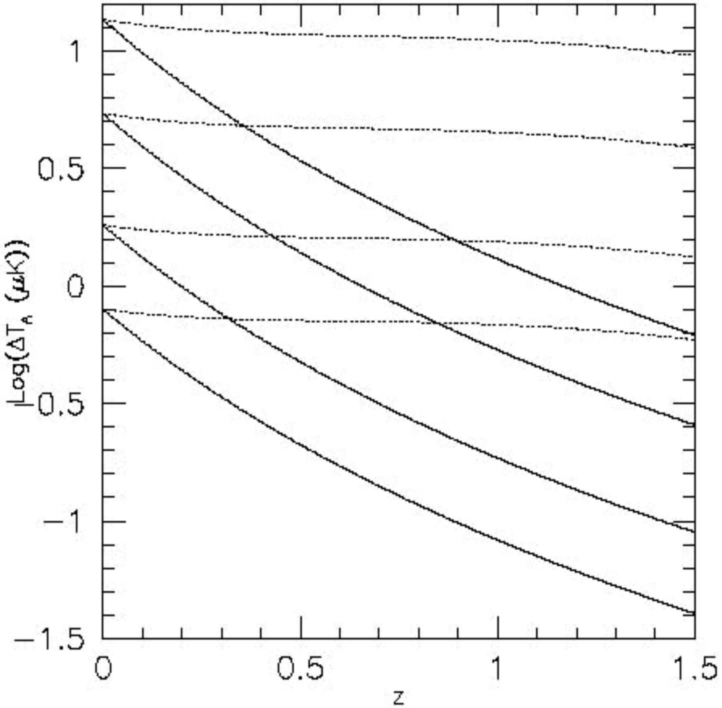

Fig. 6. Mean contamination of the SZ signal (in antenna temperature) by radio sources as a function of cluster redshift for 4 frequencies, 30, 44, 70, and 100 GHz (from top to bottom). At each frequency, the solid line refers to the case of no-evolution, the dotted line to the pure luminosity evolution models for steep- and flat-spectrum sources described in Sect. 3.4.1 of Dunlop & Peacock (1990).

from Massardi & De Zotti 2004

Angular Power Spectrum of thermal SZ effects

$$C_\ell = \int_z r^2 \frac{dr}{dz} \int_M N(M,z)\, y_\ell(M,z)\, dM\, dz$$

r = distanza comovente radiale di un cluster di massa M al redshift z

$N(M,z)$ = Funzione di massa

$y_\ell(M,z)$ = TRASFORMATA DI FOURIER ANGOLARE DI ΔT (PROFILO DI TEMPERATURA, GAS ETC ....)

❖Models exist for profiles of of temperature, density, …

❖(ex: virial equilibrium)

❖ Models for the mass function:

- ➢Press & Schechter ’74
- ➢Lee & Shandarin ’99
- ➢Sheth & Tormen ‘99

$C_l * l * (l+1)/2\pi$ has a bump @ $l \approx 10^3$ - 10^4

The power critically depends on σ_8 :
change of factor 2-3 for on σ_8 = 0.68 - 1.32

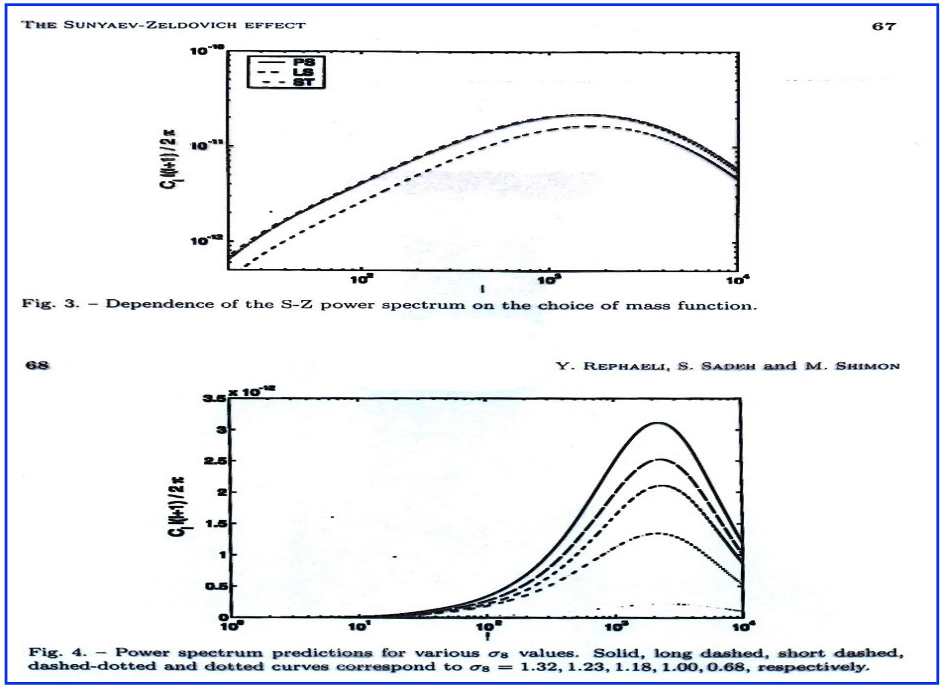

24 M. L. Norman

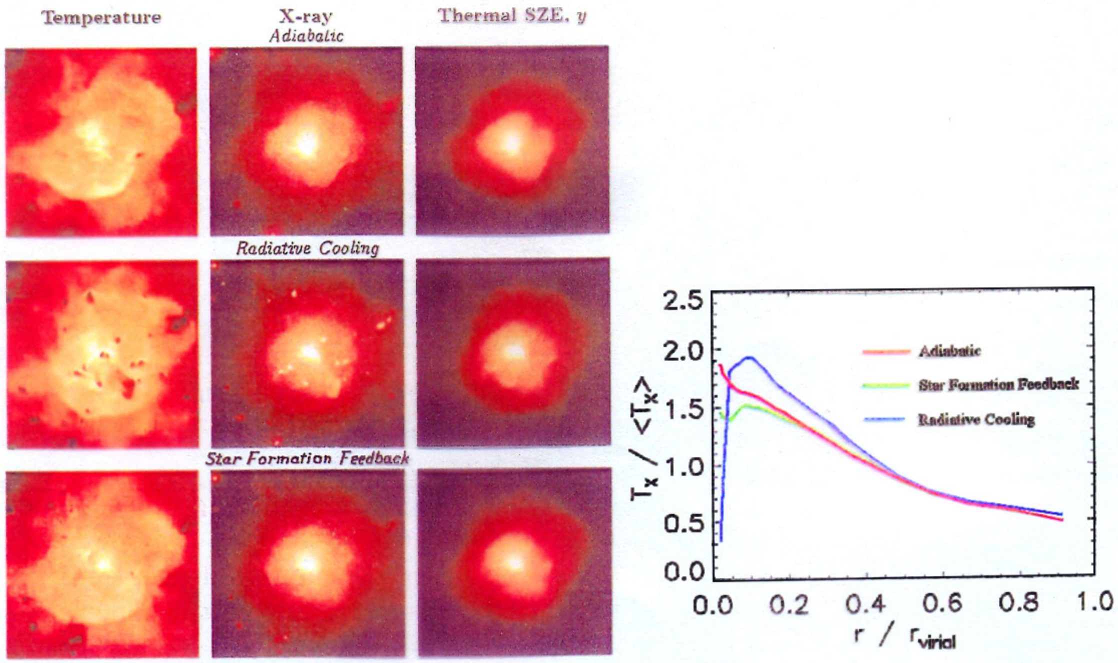

Fig. 10. – Left: columns show X-ray surface brightness, projected temperature, and Compton y-parameter for a $M = 2 \times 10^{15} M_\odot$ cluster assuming different baryonic physics. Field of view is 5 h^{-1} Mpc. Right: corresponding spherically averaged radial temperature profiles.

M. Arnaud

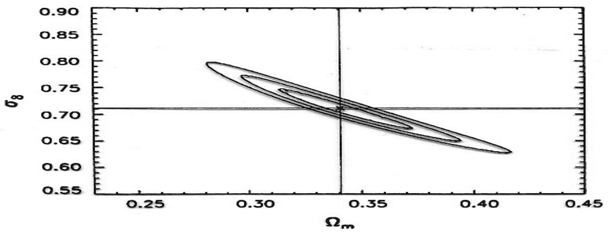

Fig. 35. – Same as fig. 34 but obtained using both cluster abundance and large-scale distribution (scale is not the same). Note the degeneracy breaking. Figure from [173].

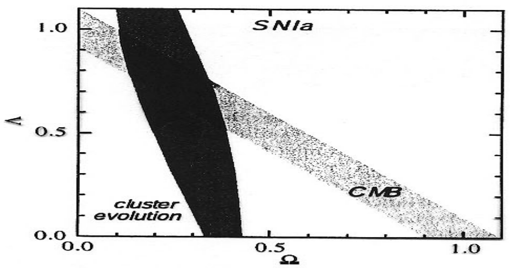

Fig. 37. – Comparison of constraints derived from the baryon mass function (fig. 33) with those from distant supernovae and the CMB (68% confidence regions). Figure from [168].

It will be also possible to study the SZ effect (both thermal and kinetic) from clusters in a statistical sense? i.e. through its contribution to the angular power spectrum, C_ℓ, of the CMB secondary anisotropies?

Ostriker J.P., Vishniac E.T., 1986, ApJ, 306, L51

Vishniac E.T., 1987, ApJ, 322, 597

Gnedin N.Y., Jaffe A.H., 2001, ApJ, 551, 3

Springel V., White M., Hernquist L., 2001, ApJ, 549, 681

da Silva A.C., et al., 2001, astro-ph/0107577

Ma C.-P., Fry J.N., 2002, PRL, 88, 211301

SKA SENSITIVITY IN TERMS OF ANGULAR POWER SPECTRUM

The statistics of temperature anisotropy is typically analyzed in spherical harmonics $Y_{\ell m}$:

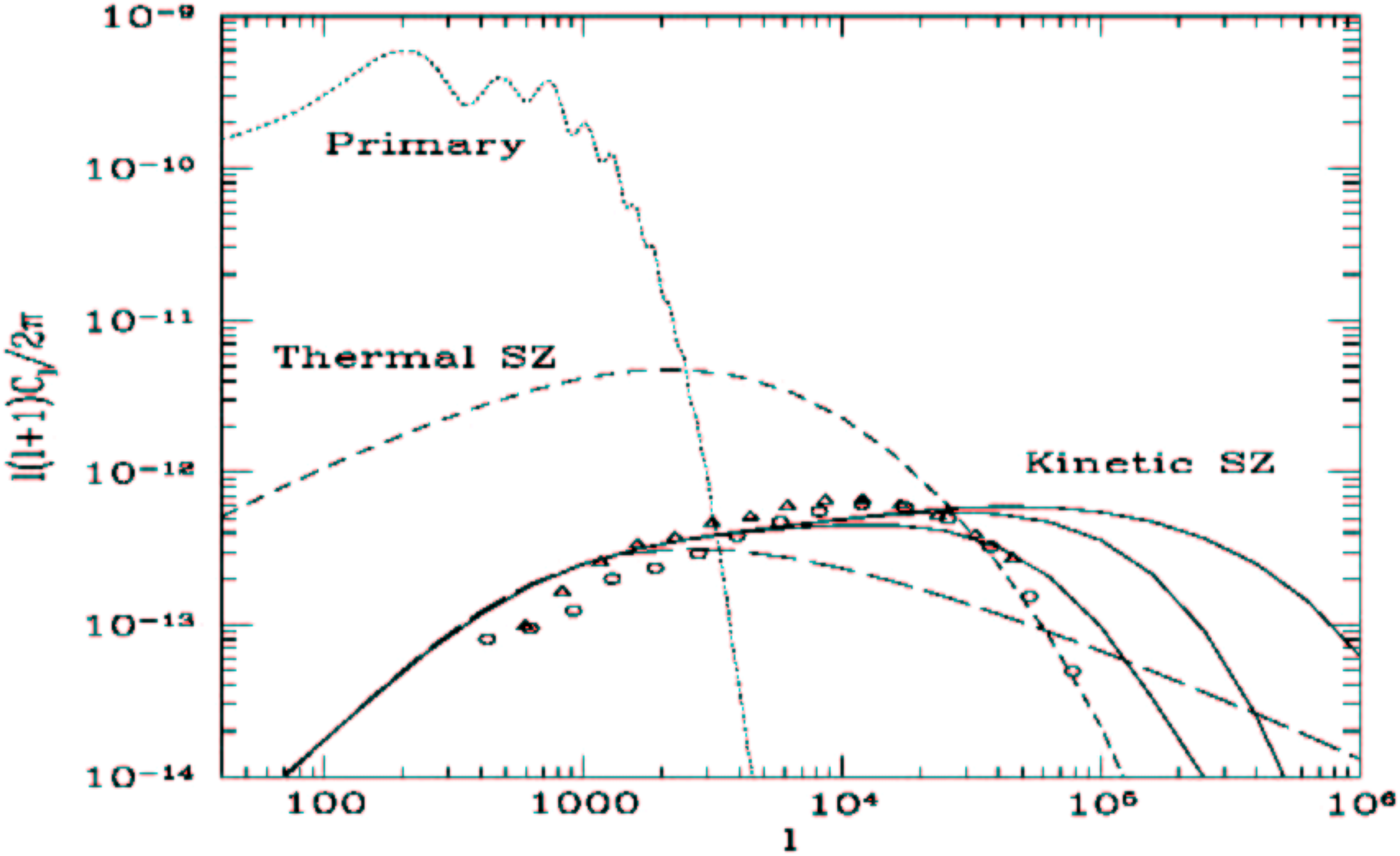

Angular power spectrum of SZ effects. From Ma C.-P., Fry J.N., 2002, PRL, 88, 211301.

SKA sensitivity to APS

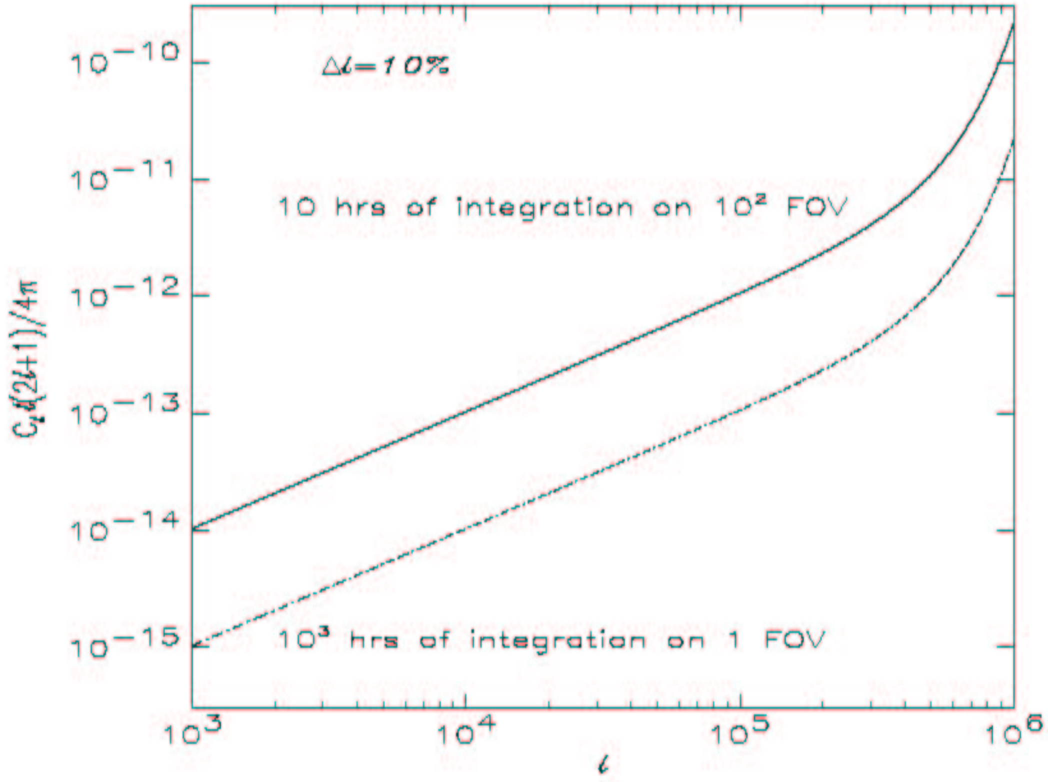

Absolute uncertainty on dimensionless CMB angular power spectrum recovery due to the instrumental noise for some reference cases.

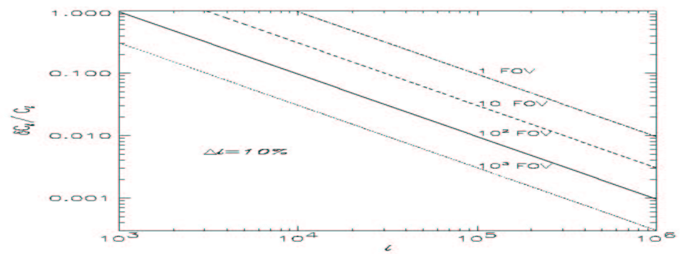

Relative uncertainty on CMB angular power spectrum recovery from combined cosmic and sampling variance for some representative sky coverages. As evident the sky coverage corresponding to $\sim 10^2$ SKA FOV (or to ~ 1 SKA FOV) allows to reach a relative "fundamental" uncertainty less than $\simeq 10\%$ at $\ell \simeq 10^4$ (or at $\simeq 10^5$) and significantly smaller at larger multipoles.

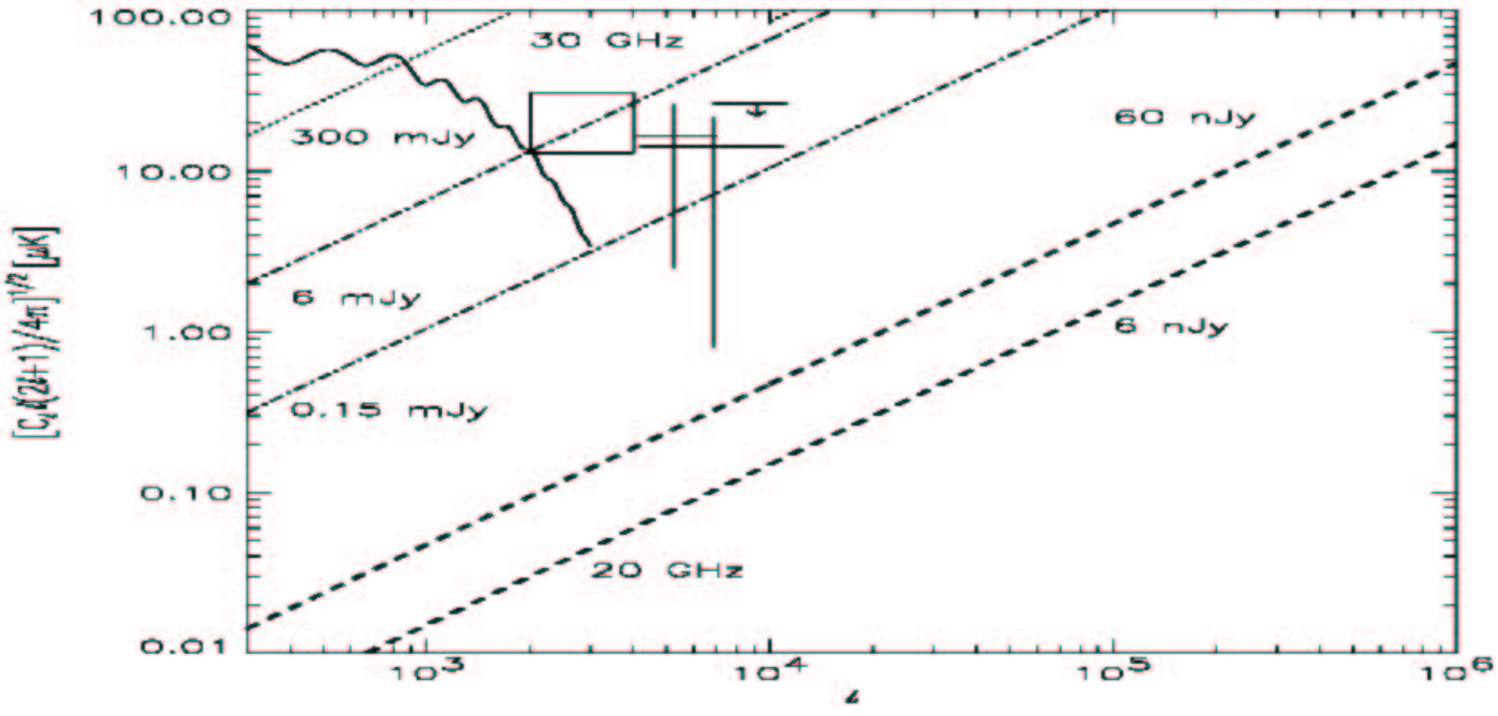

Angular power spectrum of extragalactic (mainly flat spectrum) radiosources (to be considered here as lower limit!) modelled according to Toffolatti L., et al., MN-RAS, 1998, 297, 117 compared to the CMB one and current observations.

At sub-arcmin scales (i.e. at multipoles $\ell \gtrsim 10^4$) secondary anisotropies from thermal (more important at $\ell \lesssim$ few $\times 10^4$) and kinetic (more important at $\ell \gtrsim$ few $\times 10^4$) SZ effect dominate over CMB primary anisotropy whose power significantly decreases at multipoles $\ell \gtrsim 10^3$ because of photon diffusion (Silk damping effect, Silk J., 1968, ApJ, 151, 459)

$\longrightarrow$

SZ effects angular power spectrum at $\ell \sim 10^4 - 10^5$ ($\approx 10^{-12} - 10^{-13}$ in terms of dimensionless $C_\ell \ell(2\ell + 1)/4\pi$) could be in principle investigated with the sensitivity achievable with SKA.

On the other hand, at the SKA resolution and sensitivity the contribution to fluctuations from foreground sources (both diffuse radio emission, SZ effects, and free-free emitters) at galaxy scales probably dominates over the SZ effect from clusters

SZ effect at galactic scales is also related to physical processes responsible of cosmological reionization

WMAP 7 yr results on τ

❖According to the seven-year WMAP analysis, the **current 68% uncertainty on τ is ≃ ±0.015**, almost independently on the specific model considered.

❖**Under various hypotheses**

(simple ΛCDM model with six parameters, inclusion of curvature and dark energy, of different kinds of isocurvature modes, of neutrino properties, of primordial helium mass fraction, or of a re-ionization width)

the best fit of **τ lies in the range 0.086–0.089**.

❖On the other hand, allowing for the **presence of primordial tensor perturbations or (and) of a running** in the power spectrum of primordial perturbations the best fit of **τ goes to 0.091–0.092 (0.096).**

THERMAL SUNYAEV-ZELDOVICH EFFECT AT GALAXY SCALE – $z \approx 5$

The proto-galactic gas is expected to have a large thermal energy content → detectable SZ signal

De Zotti G., et al., 2004, in Proc. Int. Symp. *Plasmas in the Laboratory and in the Universe: new insights and new challenges*, Como, September 2003, eds. Bertin G., Farina D., Pozzoli R., pg. 375, astro-ph/0401191:

1. When the protogalaxy collapses with the gas shock-heated to the virial temperature

Rees M.J., Ostriker J.P., 1977, MNRAS, 179, 541; White S.D.M., Rees M.J., 1978, MNRAS, 183, 341

2. In a later phase as the result of strong feedback from a flaring active nucleus

Ikeuchi S., 1981, PASJ, 33, 211; Natarajan P., Sigurdsson S., Silk, J., 1998, MNRAS, 298, 577; Natarajan P., Sigurdsson S., 1999, MNRAS, 302, 288; Aghanim N., Balland C., Silk, J., 2000, A&A, 357, 1; Platania P., Burigana C., De Zotti G., Lazzaro E., Bersanelli M., 2002, MNRAS, 337, 242; Lapi A., Cavaliere A., De Zotti G., 2003, ApJ, 597, L93

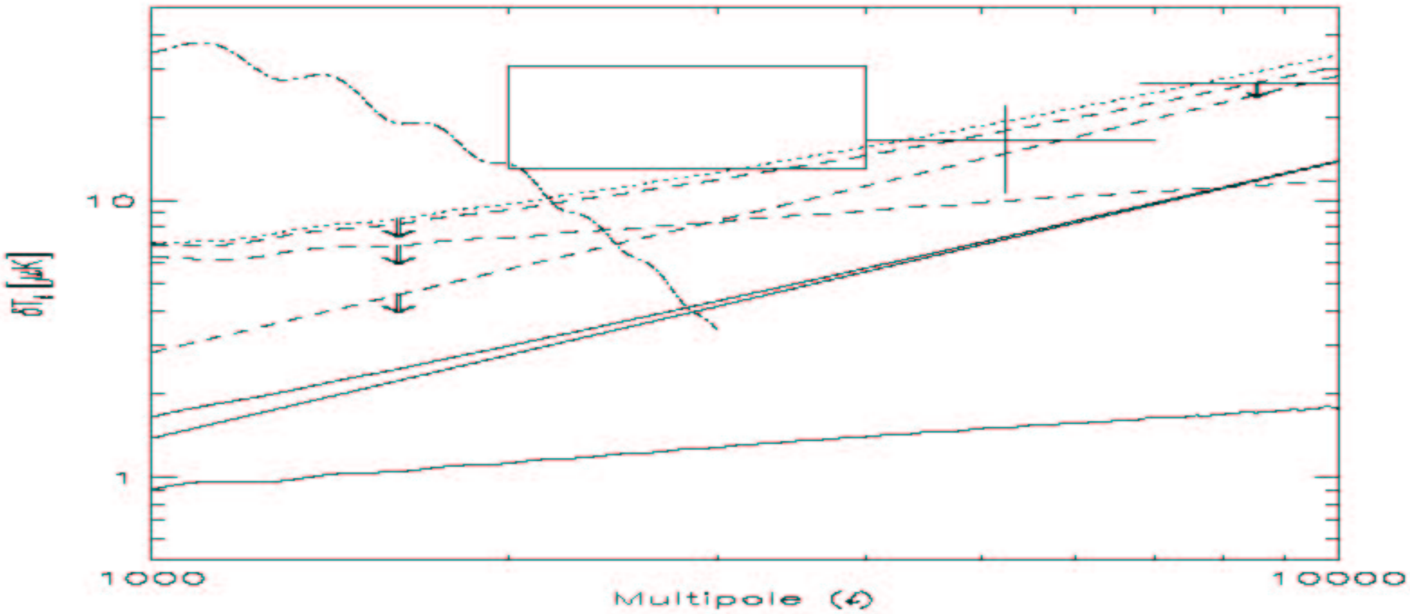

APS of SZ effects at 30 GHz vs. CMB primary fluctuation APS. CBI (Mason B.S., et al., 2003, ApJ, 591, 540, BOX) and BIMA (Dawson K.S., et al., 2002, ApJ, 581, 86, DATA POINTS). Solid lines: contributions from quasar driven blast-waves. Dashed lines: contributions from proto-galactic gas (upper limits: extreme assumption that $t_{\rm cool} = t_{\rm exp}$). Dots: overall contribution.

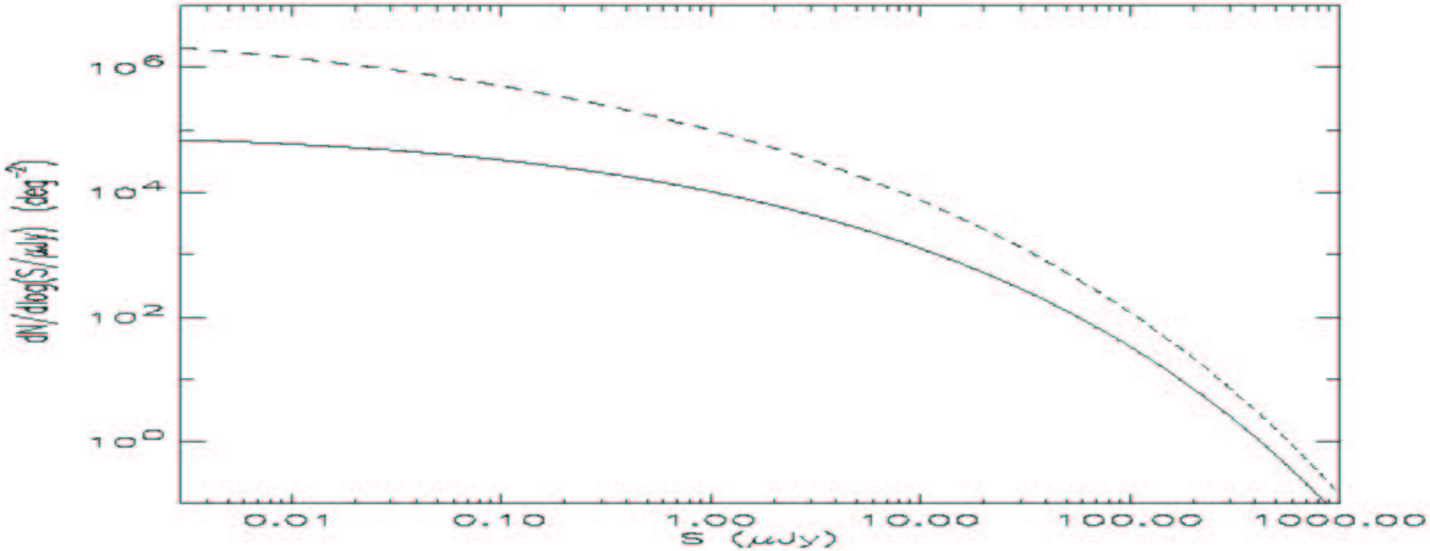

Number count predictions at 20 GHz for SZ effects as function of the absolute value of the flux from proto-galactic gas heated at the virial temperature (dashes) assuming $M_{\rm gas}/M_{\rm vir} = 0.1$ and from quasar driven blast-waves (solid line). The exponential model for the evolving luminosity function of quasars is derived by Pei Y.,1995, ApJ, 438, 623 for an optical spectral index of quasars $\alpha = 0.5$ ($S_\nu \propto \nu^\alpha$). The parameters have been set at $\epsilon_{\rm BH} = 0.1$, $f_h = 0.1$, $k_{\rm bol} = 10$, $t_{\rm q,opt} = 10^7$ yr.

Direct probe of these models and their accurate knowledge

through a precise high resolution imaging:

SKA contribution $\longrightarrow$

Number counts at 20 GHz:

In a single SKA FOV about few $\times 10^2 - 10^3$ SZ sources with fluxes above $\sim$ 100 nJy could be then observed in few hours of integration

Given the typical source sizes, we expect a blend of sources in the SKA FOV at these sensitivity levels

Much shorter integration times, $\sim$ sec, on many FOV would allow to obtain much larger maps with a significant smaller number of resolved SZ sources per FOV.

Both surveys on relatively wide sky areas and deep exposures on limited numbers of FOV are interesting and easily obtainable with SKA.

FREE-FREE EMITTERS – $z \approx 10$

Reionization (WMAP 1-yr data release) affects the CMB both in anisotropies at large and small scales and in the spectrum.

The understanding of the ionizing emissivity of collapsed objects and the degree of gas clumping is crucial for reionization models.

Observations of diffuse gas and Population III objects in thermal bremstrahlung directly probe of these quantities.

Free-free emission produces both localized and global spectral distortion of the CMB.

Diffuse Ionized IGM $\longleftarrow$ VS $\longrightarrow$ Ionized Halos

$\longrightarrow$ Observations at high resolution of dedicated sky areas – Fluctuations in the free-free background.

Model by Oh S.P., 1999, ApJ, 527, 16: halos collapse and form a starburst lasting $t_o = 10^7$ yr

then recombine and no longer contribute to the free-free background.

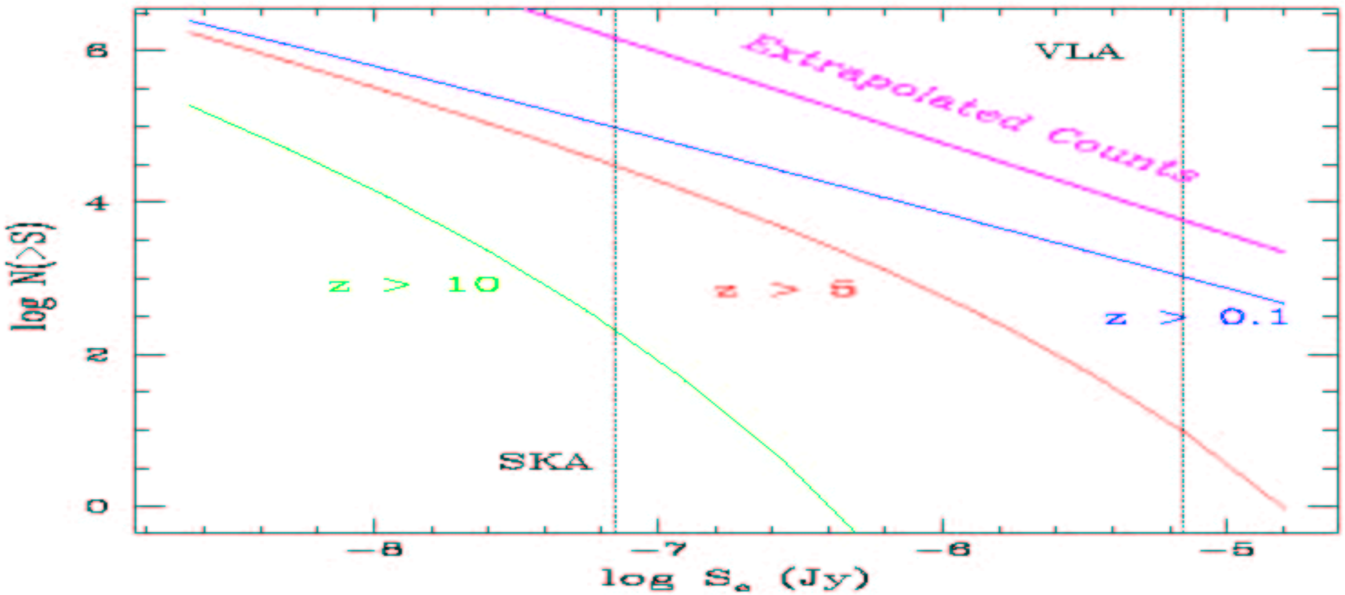

Number of sources which may be detected in the 1° by SKA, as a function of the threshold flux S_c. Realistic limiting fluxes for point source detection are shown. The extrapolated source counts from Partridge R.B., Richards E.A., Fomalont E.B., Kllerman K.I., Windhorst R., 1997 ApJ, 483, 38 are also shown. From Oh S.P., 1999, ApJ, 527, 16.

SKA should be able to detect $\sim 10^4$ individual free-free emission sources with $z > 5$ in 1 square degree above a source detection threshold of 70 nJy.

Redshift information from the Balmer line emission detectable by the Next Generation Space Telescope (NGST) $\longrightarrow$ discrimination between ionized halos from other classes of radio sources.

Ionized halos $\longrightarrow$ temperature fluctuations.

Poisson contribution is predicted to be larger (smaller) than the clustering one at scales smaller (larger) than $\sim 30''$.

On the other hand, both are likely dominated by the radio source contribution.

Integrated emission from ionized halos $\longrightarrow$ global CMB spectral distortion

$\Delta T_{ff} = c^2 \langle S \rangle / 2 k_B \nu^2$, as computed from the mean sky averaged signal $\langle S \rangle$.

By using Eq. (21) (no point source removal is feasible at degree scales) with $z_{\rm min}$ and $S_c = 0 \longrightarrow$ Free-Free distortion $\Delta T_{ff} = 3.4 \times 10^{-3}$ K at 2 GHz

$\sim$ Free-free distortion parameter $y_B \simeq 1.5 \times 10^{-6}$, well within the observational capability of DIMES (next and last topic ...)

SKA CONTRIBUTION TO FUTURE CMB SPECTRUM EXPERIMENTS – $z \lesssim 10^7$

Current limits on CMB spectral distortions and the constraints on energy dissipation processes in the plasma in the plasma (Salvaterra R., Burigana C., 2002, MNRAS, 336, 592)

$|\Delta\epsilon/\epsilon_i| \lesssim 10^{-4}$

mainly set by COBE/FIRAS

(Mather J.C. et al., 1990, ApJ, 354, L37

Fixsen D.J., et al., 1996, ApJ, 473, 576).

Need for Future CMB spectrum experiments from space

DIMES $\approx$ sensitive as FIRAS but at 0.5 cm $\lesssim \lambda \lesssim$ 15 cm

Kogut A., 1996, *Diffuse Microwave Emission Survey*, in XVI Moriond Astrophysics meeting *Microwave Background Anisotropies*, March 16-23, Les Arcs, France, astro-ph/9607100

(see also Kogut A., 2003, *Reionization and Structure Formation with ARCADE*, in the Proc. of *The Cosmic Microwave Background and its Polarization*, New Astronomy Reviews, eds. Hanany S., Olive K.A., pg. 945, astro-ph/0306044)

FIRAS II $\approx 10^2$ times more sensitive than FIRAS always at $\lambda \lesssim 0.5$ cm,

D.J. Fixsen and J.C. Mather, 2002, ApJ, 581, 817

→ Accuracy potentially able to constrain (or probably detect) energy exchanges 10–100 times smaller than the FIRAS upper limits.

PIXIE (Kogut et al. 2011) perspectives to combine CMB polarization mission with absolute calibration

→ Include in new COrE-like mission idea?

In particular, experiments like DIMES may probe dissipation processes at early times ($z \gtrsim 10^5$) resulting in Bose-Einstein like distortions quantified by the chemical potential $\mu \simeq 1.4 \Delta\epsilon/\epsilon_i$

Sunyaev R.A., Zeldovich Ya.B., 1970, Ap&SS, 7, 20
Danese L., De Zotti G., 1980, A&A, 84, 364
Burigana C., Danese L., De Zotti G., 1991, A&A, 246, 59

and free-free distortions

Barlett J.G., Stebbins A., 1991, ApJ, 371, 8

possibly generated by heating (but, although disfavoured by WMAP, in principle also by cooling mechanisms Stebbins A., Silk J., 1986, ApJ, 169, 1) at late epochs ($z \lesssim 10^4$)

Burigana C., Salvaterra R., 2003, MNRAS, 342, 543

Cosmological applications

Primordial distortions

BIG BANG — z_{term} — z_{BE} — z — z_{ric} — z today

Bose-Einstein like spectrum

$$\eta_\nu = \frac{1}{e^{(h\nu/kT)+\mu} - 1}$$

with μ function of *X*

$$\mu(x) \simeq \mu_0 \, e^{(-x_C/x)}$$

Superposition of black bodies

$$\eta(x, y^*) \simeq (4\pi y^*)^{-1/2} \int_0^\infty \eta_0(x') \exp\left[- \frac{(\ln(x/x') + 3y^*)^2}{4y^*} \right] \frac{dx}{x'}$$

where

$$y^* = \int \frac{k_B(T_e - T_\gamma)}{m_e c^2} d\tau$$

Free-free distortions

Late distortions

Related (mainly) to the reionization history of the universe

The high redshift reionization detected by WMAP

Kogut A., et al., 2003, ApJS, 148, 161

supports the existence of late coupled Comptonization distortions with $\Delta\epsilon/\epsilon_i \simeq 4y \approx$ few $\times 10^{-6}$ and free-free distortions (with a highly model dependent amplitude)

$$y(z) = \int_{1+z}^{1+z_i} (\phi - \phi_i)(kT_r/m_e c^2) n_e \sigma_T c t_{exp} \frac{d(1+z)}{1+z}$$

$$y_B(z) = \int_{1+z}^{1+z_i} (\phi - \phi_i)\phi^{-3/2} g_B(x,\phi) K_{0B} t_{exp} \frac{d(1+z)}{1+z}$$

$$K_{0B} \simeq 2.6 \times 10^{-25} (T_0/2.7K)^{-7/2} (1+z)^{5/2}$$

$$\times [\Omega_b (H_0/(50\mathrm{km/s/Mpc}))^2]^2 \mathrm{sec}^{-1}$$

Burigana C., Finelli F., Salvaterra R., Popa L.A., Mandolesi N., *On the cosmological implications of next and future CMB space experiments*, (2004), Recent Research Developments in Astronomy & Astrophysics - Vol. 2, p. 59.

Constraints or detection on/of spectral distortions

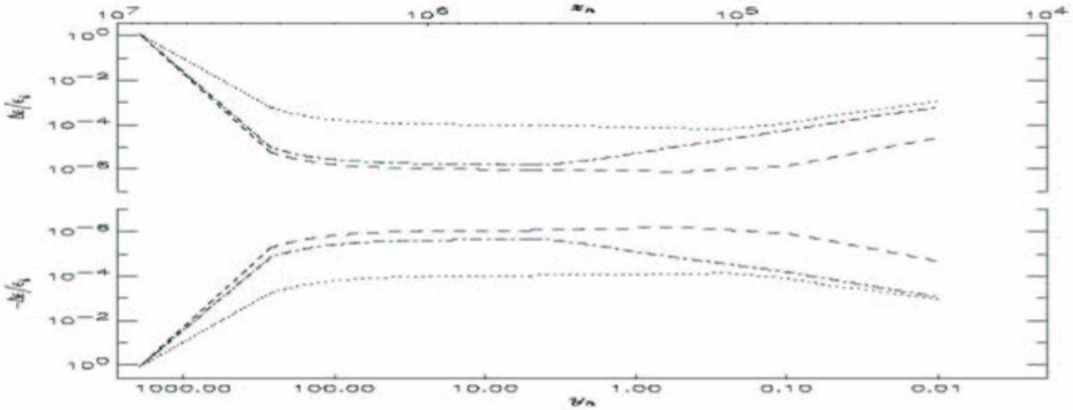

Constraints on energy dissipations at various cosmic epochs based on current data and achievable by adding future data from a DIMES-like experiment and from DIMES-like plus a FIRAS II-like experiment. From Buri- ... F., Salvaterra R., Popa L.A., Mandolesi ... mological implications of next and future ... periments, (2004), Recent Research De- ... Astronomy & Astrophysics - Vol. 2, p.

In the presence of distortions : results achievable with a new low frequency experiment

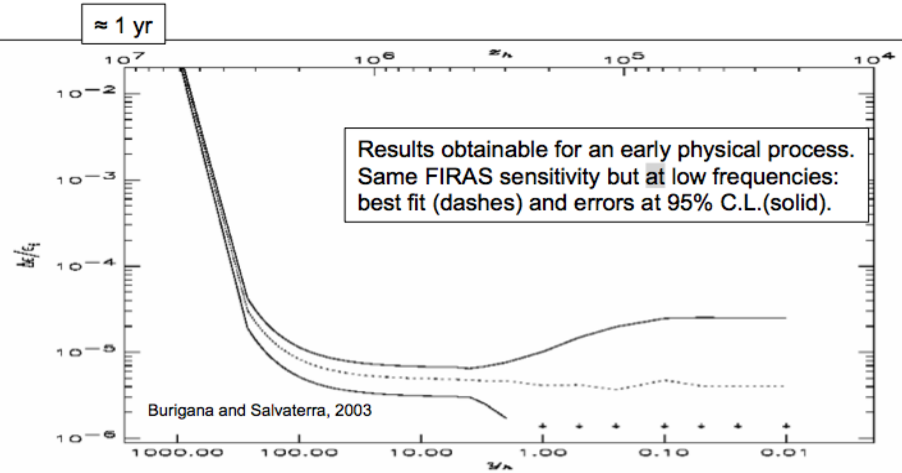

Figure 3. Constraints on the energy exchanges derived at different cosmic times by considering the case of a single dissipation process on the basis of the FIRAS data calibrated according to Mather et al. 1999 and data simulated as in the case of an energy injection with $\Delta\epsilon/\epsilon_i \geq 5 \times 10^{-6}$ and observed with a DIMES-like experiment. The dissipation epoch is assumed to be known (is the same in the generation of simulated data and in the fit). The different lines refer to the best fit result (dots) and to the upper and lower limits at 95 per cent CL (solid lines). The arrows indicate that the sign of the lower limit changes at $y_h \simeq 1$, where lower and upper error bars result to be very similar.

Theoretical CMB Spectral Distortions

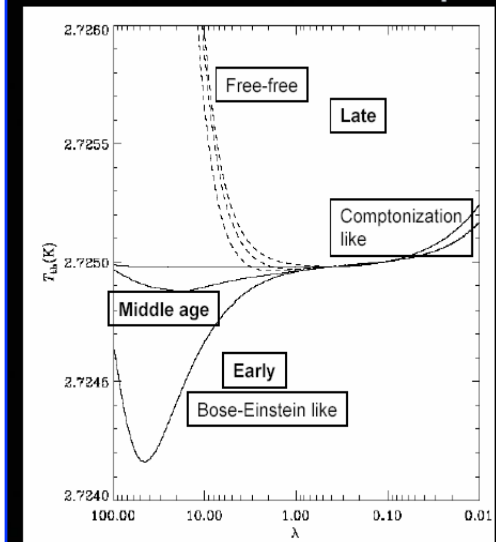

Distorted spectra in the presence of a late energy injection with $\Delta\varepsilon/\varepsilon_i = 5 \times 10^{-6}$ plus an early/intermediate energy injection with $\Delta\varepsilon/\varepsilon_i = 5 \times 10^{-6}$ occurring at y_h=5, 1, 0.01 (from the bottom to the top; in the figure the cases at y_h=5 and 1 are indistiguishable at short wavelengths; solid lines) and plus a free-free distortion with $y_B=10^{-6}$ (dashes).

To firmly observe such small distortions the Galactic and extragalactic foreground contribution should be accurately modelled and subtracted.

Galactic radio emission represents the major astrophysical problem in CMB spectrum experiments but component separation methods can in principle improved and used taking advantage from the angular dependence (angular correlation properties).

Differently from Galactic emission extragalactic foregrounds are isotropic at the angular scales of few degrees.

Recent progress on radio source counts have been presented for example in Prandoni I., et al., 2001, A&A, 365, 392 at 1.4 GHz and by Ricci R., et al., 2004, astro-ph/0407130, MNRAS, in press, at 18 GHz.

But ... the very faint tail of radio source counts is essentially unexplored and their contribution to the radio background at very low brightness temperature is not accurately known.

Ex.: by assuming differential source number counts, $N(S)$, given by $\log N(S)/\Delta N_0 \sim a \log S + b$, with $\Delta N_0 \sim 150 S^{-2.5}$ sr^{-1} Jy^{-1} (S in Jy)

(Toffolatti L., et al., MNRAS, 1998, 297, 117)

for $a \sim 0.4 - 0.6$ and $b \sim -(0.5 - 1)$

we find a contribution to the radio background at 5 GHz from sources between ~ 1 nJy and $\sim 1\mu$Jy between few tens of μK and few mK.

Signals significant at the accuracy level on CMB distortion parameters potentially achievable with experiments like DIMES.

Fit including both CMB distorted spectra and astrophysical contributions can be searched

(Salvaterra R., Burigana C., 2002, MNRAS, 336, 592)

A direct radio background estimate from precise number counts will certainly improve the robustness of this kind of analyses.

Also: ARCADE II results: questionable excess at 3 GHz interpreted as possible signature by integrated contribution from ultra-faint (high-z?) sources

→ SKA observations could certainly definitively solve this issue

- The SKA sensitivity @ 20 GHz will allow the detection
- (to 5 σ) of sources down to a flux level of:

  $\cong$ 200 (60, 20, 6) nJy

  in 1 (10, 100, 1000) hours(s) of integration over the $\cong$ 1 mas (FWHM) resolution element.

- Similar numbers

  (from 250 to 8 nJy in an integration time

  from 1 to 1000 hours, respectively)

  but on a resolution element about 10 times larger will be achieved @ $\cong$ GHz frequencies

  by using a frequency bandwidth of $\cong$ 25 %.

- → the SKA accurate determination of source number counts down to very faint fluxes can directly help the solution of one fundamental problem of the future generation of CMB spectrum space experiments @ $\lambda \geq 1$ cm.

Analysis of Galactic foregrounds

- Synchrotron emission, Faraday depolarization, 3D Galactic models
-
- Ex: see "Simulated SKA maps from Galactic 3D-emission models", by Sun & Reich 2009

  (see also Fauvet et al 2011, 2012)
  - Regular large scale magnetic field
  - Random small scale magnetic field

- Synergy with refined analyses of Planck data
- Synergy with next generation CMB polarization missions (COrE)
- Galactic foreground modelling & separation from CMB maps

CONCLUSION

- SKA is not specifically devoted to the CMB because of its high resolution and the limited high frequency coverage

  … but …

- The extreme sensitivity & resolution of SKA
  → detailed mapping of the thermal plasma properties in the intergalactic and intracluster medium and at galaxy (including Milky Way) scale:

  - Detailed mapping of the SZ effect towards cluster of galaxies
  - Number counts & imaging possibilities of the SZ effect from early quasars and protogalactic gas
  - Number counts & imaging possibilities of the free-free emission from early ionized halos
  - Contribution to the future CMB spectrum experiments devoted to the comprehension of the plasma thermal history at early epochs, through the extremely accurate control of the extragalactic radio source counts at very faint fluxes & to CMB polarization projects through better understanding of foreground emissions